Conceptual Deconstruction of the Simulated Precipitation Response to Climate Change

Christian Stassen[1], Dietmar Dommenget[1,2] and Robin Chadwick[3,4]

[1] ARC Centre of Excellence for Climate System Science, Monash University, Clayton, Australia

[2] ARC Centre of Excellence for Climate Extremes, Monash University, Clayton, Australia

[3] Met Office Hadley Centre, Exeter, United Kingdom

[4] Global Systems Institute, University of Exeter, Exeter, United Kingdom

Correspondence: Christian Stassen (christian.stassen@monash.edu)

Abstract

State-of-the-art climate change projections of the CMIP5 simulations suggest a fairly complex pattern of global precipitation changes, with regions of reduced and enhanced precipitation. Conceptual understanding of these projected precipitation changes is difficult if only based on coupled general circulation model (CGCM) simulations, due to the complexity of these models. In this study we describe a simple deconstruction of the ensemble mean CMIP5 projections based on sensitivity simulations with the globally resolved energy balance (GREB) model. In a series of sensitivity experiments we force the GREB model with four different CMIP5 ensemble mean changes in: surface temperature, evaporation and the vertical atmospheric velocities mean and its standard deviation. The resulting response in the precipitation of the GREB model is very close to the CMIP5 ensemble mean response, suggesting that the precipitation changes can be well represented by a linear combination of these four forcings. The results further provide good insights into the drivers of precipitation change. The GREB model suggests that not one forcing alone can be seen as the main driver, but only the combination of all four changes results in the complex response pattern. However, the dominant forcings are the changes in the large-scale circulation, rather than the pure thermodynamic warming effect. Here, it is interesting to note that changes in high-frequency atmospheric variability of vertical air motion (weather), that are partly independent of the changes in the mean circulation, have a control on the pattern of the time-mean global precipitation changes. The approach presented here provides a powerful basis on which the hydrological cycles of CGCM simulations can be analysed.

Key words: Climate Change, Precipitation, Hydrological Cycle, Simple Climate Model

1. Introduction

In his attempts to explain ice ages Arrhenius (1896) was the first to link variations in CO2 concentration to the greenhouse effect using basic physical considerations. Decades after him others followed using basic energy balance models to estimate the effect increasing levels of greenhouse gases have on the climate (Budyko 1972; North et al. 1981; Sellers 1969). Since the first numerical weather forecast by L.W. Richardson in the 1920 was produced by hand, the computational revolution helped develop simple energy balance models into fully complex coupled general circulation models (CGCMs) (Manabe and Stouffer 1980; Meehl et al. 2007; Meehl and Stocker 2007). Since then the main aim of model development has been to improve the physical representation of the processes in the climate system by either including more processes that have not been considered before, or by increasing the resolution of models. These CGCMs simulate processes in the ocean, on land and in the atmosphere and are therefore focusing on the most realistic and best representation of the climate system as a whole.

In recent decades increasing computer power has allowed these highly complex CGCMs to progressively increase their resolution and there is a strong interest in the research community to push the resolution of climate models to new boundaries (e.g. Haarsma et al. 2016; Marotzke et al. 2017). It has been shown that increasing the model resolution addresses a lot of common problems seen in CGCMs (Haarsma et al. 2016), such as aspects of the large-scale circulation (Masson et al. 2012; Shaffrey et al. 2009), the global water cycle (Demory et al. 2014), movements of the Atlantic inter-tropical convergence zone (ITCZ) (Doi et al. 2012) and the diurnal precipitation cycle (Birch et al. 2014; Sato et al. 2009). While expanding the scope of climate models by adding more processes and increasing the resolution, several existing problems, such as substantial precipitation biases, remain unsolved. In addition, constantly increasing the resolution and complexity of climate models does not help to gain a more conceptual understanding of climate change, as multiple processes interact with each other (Dommenget and Floter 2011).

Many aspects of climate change seen in complex CGCMs can be found in models with intermediate complexity such as CLIMBER-2 (Petoukhov et al. 1999), the UVic Earth system climate model (Weaver et al. 2001) or the simple atmosphere-ocean-sea-ice model developed by Wang and Myask (2000). In addition, idealised models such as the ω- and humidity-based model by Pendergrass and Gerber (2016) or the simple enhanced advection model by Chadwick et al. (2016) are capable of representing many aspects of the climate change response seen in complex CGCMs. Simplified climate models and energy balance considerations are capable of explaining the large-scale features of the climate system and climate change (e.g. Arctic amplification and land-sea contrast (Dommenget and Floter 2011; Izumi et al. 2015)).

One topic in climate change that deserves urgent attention is the changing pattern of the hydrological cycle (Donat et al. 2016). Changes of rainfall have direct impacts on the environment and on human health (Dai 2011; Parry et al. 2004; Patz et al. 2005). Projections of how rainfall is changing are primarily based on CGCMs simulations of the Coupled Model Intercomparison Project version 5 (CMIP5) (Taylor et al. 2012) or earlier (i.e. CMIP3 (Meehl et al. 2007)). These simulations project an increase in global mean precipitation of roughly 2% per degree of warming (Held and Soden 2006). The 2% change in precipitation comes in contrast to an increase in atmospheric water vapour of about 7% per degree of warming closely following the Clausius-Clapeyron equation. This muted response is explained by a general slowdown of the atmospheric circulation (Chadwick et al. 2013; Held and Soden 2006) and changes in radiative cooling (Allen and Ingram 2002; Pendergrass and Hartmann 2014). That is, as water vapor increases, the atmosphere cannot emit radiation at a large enough rate to support precipitation matching the rate of increase in water vapour (Stephens and Ellis

2008). Many studies have suggested that changes in radiative cooling dictate the global precipitation response and in turn control the global evaporation response, which on long time scales have to match. However, Webb et al. (2018) showed that increases in surface evaporation can have a substantial impact on radiative cooling itself. Richter and Xie (2008) looked at this muted response of precipitation from the perspective of evaporation and found that the evaporation response is mainly limited through increases in surface relative humidity and surface stability. This highlights the fact that precipitation and evaporation are closely linked and makes it a complex cycle to study.

Although precipitation is increasing by 2% per degree of warming globally, this does not mean it is increasing at the same rate everywhere. Precipitation is generally projected to increase in the ITCZ, with a large-scale precipitation decline in the subtropics and an increase in precipitation in mid- to high- latitude storm tracks (Allen and Ingram 2002; Chou and Neelin 2004; He and Soden 2016; Held and Soden 2006; Neelin et al. 2006). This pattern change is often referred to as the 'wet-get-wetter' (Held and Soden 2006). The wet-get-wetter hypothesis is mainly built on the idea that a warmer atmosphere holds and therefore transports more moisture out of dry regions into wet regions if the circulation remains unchanged (Chadwick et al. 2013). The thermodynamic response would also lead to a high correlation between the mean, control precipitation and the change of precipitation with climate change. However, Chadwick et al. (2013) have shown that on regional scales the precipitation response is poorly correlated with pre-industrial precipitation, leaving the conclusion that the dynamics are changing. There has been an observed weakening of the Walker circulation (Vecchi et al. 2006), a weakening of the Hadley cells (Lu et al. 2007; Vecchi and Soden 2007), a poleward shift of storm tracks (Bengtsson et al. 2006; Mbengue and Schneider 2017; Yin 2005) and a shift in tropical convergence zones (Chadwick et al. 2013) has been shown in GCM projections.

In this study we present a conceptual deconstruction of the CMIP5 ensemble mean precipitation changes, to better understand the climate change forcings that drive these changes. The forcings that control precipitation changes can be illustrated by a simplified sketch of the atmospheric water cycle (*Fig. 1*). Here an atmospheric volume contains a water reservoir (humidity) that is controlled by the in and out flow of water due to horizontal transport, evaporation and precipitation. Given this mass balance, precipitation changes result from changes in the humidity, horizontal transport, evaporation or in the processes that control precipitation.

We will use the Globally Resolved Energy balance (GREB) model from Dommenget and Floter (2011) with the hydrological cycle model from Stassen et al. (2019) to investigate how the CMIP5 ensemble mean projected changes in the surface temperatures, atmospheric circulation and evaporation lead to the projected changes in precipitation. We will illustrate the feasibility of this approach and discuss how the individual elements of the changing climate contribute to the projected changes in precipitation.

The following section will introduce the data, models and methods used. It will in particular discuss the GREB model and how we make use of it as an analysis tool. In section 3 the main results of this study will be presented. Finally, we give a discussion and summary of the results.

2. Data and Methods

This section provides an overview on the CMIP5 model data used. It further gives a short introduction to the GREB model, how it differs from other climate models (e.g. CGCMs) and discusses the hydrological cycle model in the GREB model, which is a key element for this study. We then explain the main analysis approach of this study: sensitivity studies with the GREB model forced by changes in the boundary conditions according to the CMIP5 RCP8.5.

CMIP data

The models of Coupled Model Intercomparison Project phase 5 (CMIP5) (Taylor et al. 2012) used in this study are summarized in *Tab.1*. We used all available models of the pre-industrial and RCP8.5 scenario that provided the variables and time frequency needed for the analysis presented in this study. All datasets are re-gridded to a horizontal resolution of 3.75° x 3.75° to match the GREB model horizontal resolution and monthly climatologies are calculated. For the climatology of ω_{mean} and ω_{std} a daily output frequency is used and an unweighted vertical mean over all levels is applied to smooth the data. The multi-model ensemble mean over all models in *Tab.1* is calculated separately for the pre-industrial and RCP8.5 scenarios and the response is defined as the difference between RCP8.5 2070-2100 period and the pre-industrial simulation. Models with more than one realization are considered by the average of all realizations (i.e. a model with one realisation and a model with many realisations are weighted equally in the multi model ensemble mean).

GREB model

The GREB model based on Dommenget and Floter (2011) and Stassen et al. (2019) is a three-layer (land, ice and ocean surface, atmosphere and subsurface ocean) global climate model on a 3.75° x 3.75° horizontal latitude-longitude grid. It has four main prognostic, tendency equations: surface temperature (T_{surf}), atmospheric temperature and specific humidity, and subsurface ocean temperatures (not relevant for this study). The model simulates thermal (long-wave) and solar (short-wave) radiation, heat and moisture transport in the atmosphere by isotropic diffusion and advection with the mean winds, the hydrological cycle (evaporation, precipitation and moisture transport), a simple ice-snow albedo feedback and heat uptake in the subsurface ocean. The tendency equations of the model are solved with a time step of 12h. For the atmospheric transport equations, a shorter time step of 0.5 h is used. The input boundary conditions for the GREB model include the typical CGCM constraints, such as incoming sunlight, topography, land-sea mask, CO2 concentrations, etc. In addition, wind, cloud cover and soil moisture fields are seasonally prescribed boundary conditions, and the tendency equation of surface temperature, deep ocean temperature and specific humidity are flux corrected towards reanalysis data. The flux corrections are calculated once and do not change in the control and sensitivity run. Additionally, surface temperature and evaporation in GREB can be forced into any mean state by prescribing them. This allows us to use the GREB model as an analysis tool, which will be a key element of this paper.
Thus, the GREB model is conceptually very different from the CGCM simulations in the Coupled Model Intercomparison Project phase 5 (CMIP5), as atmospheric circulations, cloud cover and changes to soil moisture are not simulated but prescribed as external boundary conditions. Additionally, the GREB model has no internal variability, as atmospheric fluid dynamics (e.g. weather systems) are not explicitly simulated. Subsequently, the model will converge to its equilibrium points (all tendency equations converge to zero), for the boundary conditions in this study. The control climate or response to forcings can therefore be estimated from a single year.

In the control simulations the GREB model uses climatological fields for surface temperature, specific humidity, horizontal winds and vertical winds taken from the ERA-Interim reanalysis data from 1979 to 2015 (Dee et al. 2011). The cloud climatology is taken from the International Satellite Cloud Climatology Project (Rossow and Schiffer 1991). The ocean mixed layer depth is taken from Lorbacher et al. (2006). Topographic data are taken from the ECHAM5 atmosphere model Roeckner et al. (2003). The mean vertical velocity, ω_{mean} and the daily variability, ω_{std}, used in the GREB model are shown in *Fig. 2* for the annual mean and the seasonal cycle. For more details, refer to Dommenget and Floter (2011) and Stassen et al. (2019). The performance of the GREB model in a number of different simulations and scenarios is discussed in Dommenget and Floter (2011) and Dommenget et al. (2019).

Hydrological cycle model

The hydrological cycle in GREB (Stassen et al. 2019) consists of three models calculating precipitation, evaporation and circulation of water vapour in the atmosphere. Soil moisture is a seasonally varying prescribed boundary condition. Precipitation, Δq_{precip}, is diagnosed in the model based on four environmental factors: the actual simulated specific humidity, q, the relative humidity, rq, calculated as ratio using the saturation specific humidity as function of temperature and scaled by topographic height (Dommenget and Floter 2011), in the GREB model and the prescribed boundary condition of ω_{mean} and ω_{std}.

$$\Delta q_{precip} = r_{precip} \cdot q \cdot \left(c_q + c_{rq} \cdot rq + c_{\omega} \cdot \omega_{mean} + c_{\omega std} \cdot \omega_{std}\right) \qquad [1]$$

The model parameters, r_{precip}, c_q, c_{rq}, c_{ω} and $c_{\omega std}$ were fitted to minimise the root mean square error between observations and the GREB simulated precipitation (see *Tab. 2* for the values). According to this model precipitation is proportional to the atmospheric moisture (q) and it is stronger for larger relative humidity (rq), mean upward atmospheric motion (ω_{mean}) and for larger variability in the upward atmospheric motion (ω_{std}). It needs to be considered here that the precursors for precipitation are in general not dynamically independent (i.e. relative humidity and ω_{mean} are correlated Singh et al. (2019)). Further, this model does parameterise precipitation in a climate model without weather fluctuations, that are typically simulated within CGCMs. Thus, these parameterisations do capture the effect of weather fluctuations indirectly, in particular the last term (ω_{std}) is a representation of weather fluctuations.

The GREB model simulated precipitation and its seasonal cycle for control conditions are shown in *Fig. 2 a and b*. The precipitation annual mean and seasonal cycle of this model is actually closer to the observed than most CMIP5 simulations (Stassen et al., 2019). This good performance relative to CMIP5 models indicates that precipitation is primarily a result of the environmental factors controlling it. Since CMIP5 models do have significant biases in each of these environmental controlling factors, in particular in the mean vertical circulation, the resulting precipitation simulation of these models is biased too.

Evaporation uses a refined Bulk formula considering differences in the sensitivity to winds between land and oceans and an estimate of wind magnitudes.

$$\Delta q_{eva} = {r_{qviwv}}^{-1} \cdot \rho_{air} \cdot c_{eva} \cdot c_{w} \cdot |u_{*} + c_{turb}| \cdot \vartheta_{\mathrm{soil}} \cdot (q - q_{sat-skin}) \qquad [2]$$

The constant c_{eva} modifies the evaporation efficiency for a given mean wind speed, u_{*}, and $q_{sat-skin}$ considers an increased surface temperature to mimic the skin temperature. It reflects that the GREB model does not simulate the daily cycle of surface temperature. The parameters c_{eva} and c_{turb} were fitted against observations for ocean and land points individually to minimise the RMSE (Stassen et al. 2019).

Moisture transport, q_{crcl}, can be split into two separate terms, a transport with mean winds against a gradient in moisture $\overline{\mathrm{u} \cdot \nabla \mathrm{q}}$, and a convergence or divergence of moisture transport $\overline{\mathrm{q}\nabla \cdot \mathrm{u}}$. Moisture convergence, as it occurs for example in the ITCZ, plays the dominant role in large-scale moisture transport. In the GREB model it is approximated by knowing the vertical air flow, assuming continuity and hydrostatic balance:

$$\overline{q\nabla \cdot \mathrm{u}} \approx q \cdot f \cdot \frac{dt_{crcl}}{z_{vapour} \cdot \rho_{air} \cdot g} \cdot \omega_{mean} \qquad [3]$$

With the known parameters of water vapour scaling height, z_{vapour}, density of air, ρ_{air}, gravitational acceleration, g, and the circulation time step, dt_{crcl}. The scaling factor, $f = 2.5$, may be influenced by the coarse horizontal resolution and the single layer approximation of the GREB model (Stassen et al. 2019). There is no convergence or divergence for the temperature equation in the GREB model and therefore no direct influence of ω_{mean} on the temperature. Indirectly the temperature can be influenced by ω_{mean} through changes in moisture content and latent heating caused by precipitation.

GREB sensitivity experiments

The main analysis part of this study is based on a series of sensitivity experiments with the GREB model. For these experiments we use the ability of the GREB model to respond to changes in the boundary conditions and to control the mean T_{surf}. For the study of the precipitation response to changes in environmental factors (*eq. [1]*) the key controlling factors are the boundary conditions of ω_{mean}, ω_{std}, and the model variables q and rq.

If the precipitation is free to respond, then q and rq are largely controlled by the evaporation (Δq_{eva}; *eq. [2]*) and the atmospheric temperatures. The latter is strongly linked to T_{surf}. Thus, to study the precipitation response to changes in environmental factors, the GREB model can be driven by changes in ω_{mean}, ω_{std}, Δq_{eva} and T_{surf}. The model will respond to these changes in boundary conditions by simulated changes in the atmospheric temperature, humidity and subsequently the relative humidity. These changes will then lead to changes in precipitation following from *eq. [1]*. The annual mean values and the seasonal cycle of the key drivers, ω_{mean}, ω_{std} and Δq_{eva} are shown in *Fig. 2* and the control precipitation is shown in *Figs. 2 a and b*.

For the control simulations the GREB model is run with observed boundary conditions, as described above, and q and T_{surf} are free to evolve. For the sensitivity experiments we add the anomaly values of ω_{mean}, ω_{std}, Δq_{eva} and T_{surf} from the CMIP5 RCP8.5 ensemble mean to each of the control forcings for one or all boundary conditions while the remaining boundary conditions are kept at control values. Thus, in these sensitivity experiments Δq_{eva} and T_{surf} are not free to evolve but are prescribed by the CMIP5 RCP8.5 ensemble mean values. Atmospheric temperatures, humidity and precipitation are free to respond. Because the surface temperature is prescribed the GREB model is not very sensitive to the actual CO2 concentration. The difference between control and sensitivity simulations are defined as the response to the CMIP5 RCP8.5 ensemble mean forcings.

3. Precipitation Response to Climate Change Deconstruction

In this section we discuss the large-scale response of precipitation to changes in T_{surf}, Δq_{eva}, ω_{mean} and ω_{std} in the ensemble mean CMIP5 RCP8.5 based on the GREB sensitivity experiments (see section above). We start the discussion with illustrating the concept and then focus on how each of the four forcings contribute to the change in precipitation.

Fig. 3 shows annual mean and seasonal cycle of the four different forcings for the ensemble mean CMIP5 RCP8.5 changes. T_{surf} shows the well-known pattern of stronger warming over land, high latitudes and during winter time. Evaporation is mostly increasing over oceans and has some locations with significant decrease. The seasonal signature of the evaporation changes is fairly complex, but are somewhat marked by reduced increase in evaporation during summer time.

Changes ω_{mean} in are marked by strong increase in upward motion over the central and eastern equatorial Pacific together with a fairly complex seasonal cycle change. For the tropical and subtropical regions outside the tropical Pacific regions the changes in ω_{mean} are mostly a weakening of the mean state (e.g. increase in ω_{mean} where ω_{mean} is negative and decrease in ω_{mean} where ω_{mean} is positive). However, overall the changes in ω_{mean} do not project strongly on the control mean state (see Tab. 3).

ω_{std} strongly increases in the equatorial Pacific, mostly decreases in the subtropics and increases in the Southern Ocean. The seasonal cycle changes are similar in both hemispheres with increased variability in the subtropics and decreased variability in the mid-latitudes in summer relative to winter. It is important to note here, that the regional difference in change of ω_{std} do not match the changes in ω_{mean} outside the tropical Pacific area.

The GREB model response of the precipitation to these four forcings is shown in Fig. 4 for the annual mean and the seasonal cycle. It compares very well with the ensemble mean CMIP5 response (Fig. 4a and e). The pattern correlation and amplitude of the annual mean and seasonal cycle of the GREB model is closer to the ensemble mean CMIP5 response than most CMIP5 models, indicating that the GREB model is representing the precipitation response in the CMIP5 ensemble well (*Fig. 5)*. It further suggests that the ensemble mean CMIP5 precipitation response can be well understood in the context of the GREB model (*eq. [1]*) forced by the changes in the four environmental variables (T_{surf}, $\Delta q_{eva}, \omega_{mean}$ and ω_{std}). In the next steps we will force the GREB model with only one environmental variable at a time, while keeping the others at control values. This will illustrate how each of the four forcings contribute to the precipitation changes. We will finish this section with a discussion of the relative role of each of the four forcings.

Surface temperature changes

We start with the T_{surf} forcing, as it is the most robust forcing of climate change (Fig. 3a and b). Given that evaporation is kept at control values, the global mean precipitation cannot change, as it is in direct balance with evaporation at the global scale. However, it can have regional changes. In the GREB model the increase in T_{surf} leads to an enhanced annual mean precipitation in the ITCZ and mid- to high latitudes and decreases precipitation in the subtropical dry zones in the annual mean (*Fig. 6a*). The annual mean response pattern compares well to the annual mean control precipitation in GREB (*Fig. 2a*) and has a correlation of 0.62 (*Tab. 5*). It thus fits moderately well with the concept of the wet-get-wetter.

The increased T_{surf} leads to an increase in atmospheric temperature (not shown), which initially, while the atmospheric humidity has not responded yet, leads to a strongly decreased relative humidity in the atmosphere. This in turn initially reduces the precipitation (see *eq. [1]*). Given the unchanged evaporation, the atmospheric humidity will start to increase until a new equilibrium between precipitation and evaporation is reached. This new equilibrium is at higher atmospheric humidity (*Fig. 7d*, but lower relative humidity (*Fig. 7e*). The latter changes reflect the now more effective precipitations terms in eq. [1], as they are all proportional to the atmospheric humidity (q), see *Figs. 8d, e, f.*

The increase in atmospheric humidity, increases the atmospheric moisture transport (*Fig. 7f*), as the moisture transport is directly proportional to the atmospheric humidity (eq. [3]). The pattern of the changes in moisture transport is identical to the overall changes in precipitation (compare *Fig. 6a with 7f*) with a correlation of 1.0 (*Tab. 5*). This is by construction the case, as evaporation is unchanged and any change in precipitation has then to come from changes in moisture transport. Thus, the precipitation changes due to T_{surf} forcing lead to enhanced moisture transport that enhance precipitation in moisture convergence zones and reduces precipitation in regions with diverging moisture transport.

The same arguments hold for the changes in the seasonal cycle of precipitation. The response pattern shows an amplification of the control precipitation (compare *Fig. 2b* and *Fig. 6b*). Specific humidity increases more in winter than in summer (*appendix Fig. S1a*) and this amplification of the seasonal cycle of specific humidity leads to an enhanced seasonal transport (*Fig. S1c*). The enhanced seasonal transport of moisture supplies the enhanced seasonal precipitation.

Evaporation changes

On the global scale, changes in precipitation must equate to changes in evaporation, to maintain the atmospheric moisture mass balance. Therefore, precipitation changes cannot in principle be separated from evaporation changes in the GREB model. Here, it is interesting to note that the overall global pattern of precipitation (*Fig. 4a*) and evaporation changes (*Fig. 3c*) are fairly dissimilar (r=0.13, *Tab. 4*) despite the global constraint that the two have to be the same. This indicates, that the processes that control precipitation and evaporation on the local scale are fairly different. It is therefore useful to consider evaporation changes as a forcing for the precipitation on regional scales.

In the GREB model simulations the evaporation forcing, with all other forcings unchanged, leads to a global increase in annual mean precipitation with the largest increase in the tropics and sub-tropics (*Fig. 6c*). Only a few regions (e.g. Greenland) experience a decrease in annual mean precipitation. The response pattern is very similar to the evaporation pattern (r=0.82, see *Tab. 4*). Thus. the response in precipitation appears to be a direct local response to the evaporation forcing over oceans. Over land this direct relationship is weaker.

Since atmospheric temperature is not changing, the atmosphere cannot take up more moisture (*Figs. 7g and 7h*), therefore any increase in evaporation has to immediately precipitate locally. This is further supported by the moisture terms of the precipitation parameterisation (*eq. [1]*), which are sensitive to increases in moisture and is the main driver of the precipitation response (*Fig. 8g),* whereas the other two terms contribute little. As the water vapour in the atmosphere does not increase much, relative humidity is changing only marginally in the tropics and subtropics. The seasonal cycle changes of precipitation follow the same arguments.

While the global pattern of evaporation changes has very little relation to the global pattern of precipitation changes in the fully forced GREB model (r=0.13, *Tab. 4*), the global mean evaporation changes do control the global mean precipitation changes (or vice versa). Here it is remarkable that the overall evaporation changes (*Fig. 3c*) are only about 2% per degree global warming. This is much less than the 7% per degree global warming expected from the simple thermodynamic Clausius–Clapeyron relation, assuming eq. [2] with no circulation changes and unchanged atmospheric relative humidity. Thus, the evaporation changes appear to be strongly affected by dynamical changes in the atmospheric circulation. See also discussion in Richter and Xie (2008).

Mean vertical velocity changes

Mean vertical velocity (ω_{mean}) in GREB has two main effects. It affects precipitation directly through the parameterisation (*eq. [1]*) and indirectly through the transport of moisture (*eq. [3]*) which in turn plays a role in the precipitation parameterisation through specific and relative humidity. The forced annual mean CMIP5 RCP8.5 change in the ω_{mean} boundary condition shows a strong increase in the tropical Pacific ascending motion and a general weakening of the subtropical descending motion (*Fig. 3e*). However, the Maritime Continent shows weaker ascent compared to control. The precipitation response pattern in GREB (*Figs. 6e and f*) compares well to the pattern in the ω_{mean} change (*Figs. 3e and f*; r=-0.86 see *Tab. 4*), indicating that the precipitation changes are a direct response to the circulation changes. This is reflected in the precipitation terms, $precip_{moisture} = r_{precip} \cdot q \cdot \left(c_q + c_{rq} \cdot rq\right)$, $precip_{\omega mean} = r_{precip} \cdot q \cdot c_{\omega} \cdot \omega_{mean}$, $precip_{\omega std} = r_{precip} \cdot q \cdot c_{\omega std} \cdot \omega_{std}$ (*Figs. 8j, k, l*), which only show changes in the $precip_{\omega mean}$ term and little changes in the other two terms. It is also illustrated by the small changes in humidity and relative humidity (*Fig. 7j and k*) and the clear changes in moisture transport (*Fig. 7l*). As in the previous sensitivity experiment the surface temperature is forced to stay at control values allowing the atmosphere not to take up much more moisture before reaching saturation and therefore keeping humidity nearly unchanged. Thus, the precipitation changes are the combined effect of changes in $precip_{\omega mean}$ term of *eq. [1]* and the changes in moisture transport that both work in the same direction.

Vertical velocity variability

The ω_{std} boundary condition affects precipitation directly through *eq. [1]*. The precipitation response in GREB to this sensitivity experiments roughly matches the external boundary forcing of ω_{std} (compare *Figs. 3g and 6g*) with a correlation coefficient of 0.68 (*Tab. 4*). There is an increase in annual mean precipitation in the tropical Pacific, generally decreasing precipitation in the subtropics and small to no changes in higher latitudes, especially in the southern hemisphere.

Although ω_{std} only acts through the precipitation parameterisation it has a strong effect on specific humidity (*Fig. 7m*) and water vapour circulation (*Fig. 7o*). A decrease of ω_{std} leads to a decrease in precipitation in these areas. Since evaporation is at control values and precipitation decreased, moisture will accumulate and humidity increases. The opposite holds for the tropical Pacific where an increase in vertical velocity variability leads to more precipitation and depletes moisture. The general increase in specific humidity increases the moisture terms of the precipitation equation (eq. [1]; *Fig. 8m*) and affects the moisture circulation (*eq. [3]*) which counteracts the accumulation of moisture and transports moisture from the subtropics into the tropical Pacific (*Fig. 7o*). This change in moisture transport then supplies the water vapour needed to keep up the changes in precipitation.

Superposition

All four sensitivity experiments described above (T_{surf}, evaporation, ω_{mean} and ω_{std}) are added together in a linear superposition to evaluate if they sum up to the fully forced GREB model precipitation response in the annual mean and the seasonal cycle (*Figs. 4e and 4f*). The superposition is close to the fully forced GREB model precipitation response and to the CMIP5 response in both the annual mean and seasonal cycle patterns (*Fig. 5*), suggesting that we can think of the precipitation response as a linear combined effect of the four individual forcings. This is somewhat surprising, considering the non-linear nature of precipitation processes.

It is further remarkable that none of the four individual forcings dominate the total precipitation response (*Fig. 5*). The total precipitation is indeed a clear combination of all four forcings. The annual and seasonal cycle precipitation response is most strongly related to the changes in ω_{mean}, indicating that atmospheric circulation changes are the main drivers of the precipitation changes. The thermodynamic warming effect

(T_{surf}) has a somewhat weaker contribution to the total precipitation changes, suggesting that the thermodynamic, wet-get-wetter, processes are less important than dynamical changes.

Changes in the evaporation patterns are less correlated with the patterns of precipitation changes (*Fig. 5*), but they do control the global mean precipitation changes (which are not evaluated by *Fig. 5*), as the global moisture mass balance is a direct balance between total precipitation and evaporation. Thus, the processes of evaporation changes are essential for understanding the precipitation changes.

An alternative and simplified presentation of the combined precipitation and evaporation changes is the zonal mean precipitation minus evaporation (p-e) changes, which gives a good presentation of the large-scale changes (*Fig. 9*). The main changes in the zonally averaged CMIP5 ensemble can be described by the wet-get-wetter idea: increase in p-e near the wet equator, decrease in the dry subtropics and increase in the wet higher latitudes. This main signature is captured by both the GREB model with all forcings and by the superposition of the GREB model forced with individual forcings. However, the GREB model does overestimate the equatorial response and does underestimate the higher latitudes response, which might be related to a too weak poleward transport in the GREB model.

When we look at how each of the individual forcings contribute to this zonal p-e pattern, it is interesting to note that all four elements contribute to it. Most similar to the overall structure, though, comes from ω_{std}, indicating that changes in the atmospheric variability contribute to this p-e pattern. However, GREB does have some limitations when compared to the CMIP5 ensemble mean response. GREB is too wet in the ITCZ and the decrease of precipitation in the subtropics is too weak (*Fig. 9*). In the mid- to high-latitudes on both hemispheres GREB does not capture the drying that can be seen in CMIP5.

4. Summary and discussion

In this study we used the simple climate model GREB to decompose the CMIP5 simulations response of precipitation to climate change. The simplicity of the GREB model allows us to force single aspects of the climate system to change according to the CMIP5 ensemble mean response while other aspects remain at control values.

We presented the precipitation changes as the result of four different forcings: surface temperature, evaporation, mean circulation and circulation variability changes. The four different forcings of precipitation changes add almost linearly in the GREB model, while still giving a good representation of the changes in the CMIP simulations. This suggests that the CMIP precipitation changes can, to a large part, be considered as linear superposition of these four forcings. The effect of each of the four forcings is illustrated in the sketch of *Fig. 10*. The main findings of each of the four forcings can be summarised as follows:

Surface temperature: The increase in surface temperature, with the directly associated increase in atmospheric temperature, results in an increase in atmospheric humidity (*Fig. 10a*). This intensifies the atmospheric transport of humidity, which increases precipitation in convergence zones and decreases precipitation in divergence regions. This is the wet-get-wetter principle. In this direct effect of atmospheric warming, the surface warming pattern has little to no effect on the pattern of precipitation changes, as the latter is primarily a reflection of the mean atmospheric circulation state. However, in reality the surface warming pattern does have an important control on the atmospheric circulation changes, which do affect precipitation changes more strongly than the direct warming effect. Further the atmospheric circulation changes induced by the warming pattern do also affect the evaporation changes (Richter and Xie 2008).

Evaporation: In the absence of any other changes, an increase in evaporation leads to a direct local increase in precipitation (*Fig. 10b*). However, the more important control of evaporation is on the global scale, as global precipitation is directly balanced by global evaporation changes. Here is it interesting to note that global evaporation is only increasing by about 2% per degree global warming, exactly balancing the global precipitation changes by construction. This is in contrast to the +7% per degree global warming that would be expected from the evaporation bulk formula eq. [2], if there are no circulation and no relative humidity changes. This is also what the GREB model would simulate in response to CO_2 or surface warming forcing if no circulation changes are imposed (not shown; see also Stassen et al. 2019). While precipitation and evaporation are balanced on a global scale, it is unclear which of the two processes is forcing the muted 2% increase per degree global warming. The differences in the evaporation and precipitation patterns in both the mean state and the changes suggest that the processes controlling them are different. The strong impact of circulation and relative humidity changes on the evaporation (Richter and Xie 2008) therefore suggest that studying the processes that control evaporation changes could be essential for understanding precipitation pattern changes. Future studies, using the GREB model or otherwise, need to focus on the conceptual understanding of the processes that control future evaporation changes.

Mean circulation: Changes in the mean circulation affect the precipitation in two ways: they change the atmospheric transport of the humidity (*Fig. 10c*) and they change the precipitation directly by the parameterisation *eq. [1]*. Both combine to increase (decrease) precipitation in regions with increased convergence (divergence). The change in mean circulation is the single most important direct effect of the four forcings. This is consistent with previous studies using GCM data, which have emphasised the importance of dynamic rather than thermodynamic drivers of precipitation change at regional scales (Chadwick et al. 2013; Kent et al. 2015; Muller and O'Gorman 2011; Seager et al. 2010). Circulation changes also affect precipitation changes indirectly by affecting the evaporation changes, which further increases the importance of atmospheric circulation changes.

Circulation variability: In the GREB model the effect of weather variability on precipitation is parameterised in *eq. [1]* by ω_{std}. A decrease (increase) in ω_{std} directly decrease (increases) precipitation. In the absence of any other changes (e.g. no evaporation changes) it does increase (decrease) the atmospheric humidity and subsequently increase (decrease) the atmospheric moisture transport (*Fig. 10d*). In the context of time-mean precipitation changes this effect has not been discussed much in the literature, although Vecchi and Soden (2007) discussed a reduction in the daily omega variability in the context of the weakening of the tropical circulation. Pendergrass and Gerber (2016) also found a decrease of standard deviation of the daily vertical velocity distribution. Weller et al. (2019) found that the ω_{std} response might be related to a decrease in low-level convergence lines. Further, the study of Richter and Xie (2008) suggests that in reality the ω_{std} will also affect the evaporation. In particular, the reduction of ω_{std} in the subtropical ocean regions (*Fig. 3g*) has a high potential of affecting evaporation, as it is the region where evaporation is strongest (*Fig. 2c*). This suggest that studying changes in high-frequency (weather) variability may be important to understand large-scale precipitation and evaporation changes.

A combined effect of the warming (T_{surf}) and changes in the weather variability (ω_{std}) is that the relative importance of the different precipitation terms in *eq. [1]* are changing (see *Fig. 8a-c*). This suggests that the importance of the steady, thermodynamic, precipitation is decreasing (*Fig. 8a*), while the importance of precipitation associated with weather variability is increasing (*Fig. 8c*). Thus, the nature of precipitation is changing globally (e.g. extreme precipitation increases by 7%/K (Ban et al. 2015; Muller et al. 2011) while mean precipitation is radiatively constrained (i.e. Allen and Ingram (2002)).

The focus of this study was the conceptual understanding of projected precipitation changes. However, this study also introduced a new approach of analysing precipitation changes by using the GREB model as a diagnostic tool. The study has shown that this approach is indeed capable of analysing the projected precipitation change of the CMIP model with a focus on understanding the processes forcing these changes. This approach can also be used to understand problems in the CMIP model simulations to simulate the mean climate or to understand the diversity in the future CMIP projections of the hydrological cycle changes.

Acknowledgements

This study was supported by the Australian Research Council (ARC), with additional support coming via the ARC Centre of Excellence in Climate System Science (CE110001028) and the ARC Centre of Excellence in Climate Extremes (CE170100023). We want to thank NCI for providing computational support and resources. Robin Chadwick was supported by the Newton Fund through the Met Office Climate Science for Service Partnership Brazil (CSSP Brazil).

We would also like to thank both reviewers and the editor for the effort and time spent on carefully reading the manuscript and their thoughtful comments which helped to improve this work.

References

Allen MR, Ingram WJ (2002) Constraints on future changes in climate and the hydrologic cycle Nature 419:224-+ doi:10.1038/nature01092

Arrhenius S (1896) On the influence of carbonic acid on the air temperature of the ground Philos Mag S5:237-276

Ban N, Schmidli J, Schar C (2015) Heavy precipitation in a changing climate: Does short-term summer precipitation increase faster? Geophys Res Lett 42:1165-1172 doi:10.1002/2014gl062588

Bengtsson L, Hodges KI, Roeckner E (2006) Storm tracks and climate change J Climate 19:3518-3543 doi:Doi 10.1175/Jcli3815.1

Birch CE, Marsham JH, Parker DJ, Taylor CM (2014) The scale dependence and structure of convergence fields preceding the initiation of deep convection Geophys Res Lett 41:4769-4776 doi:10.1002/2014gl060493

Budyko MI (1972) Future Climate Eos T Am Geophys Un 53:868-& doi:DOI 10.1029/EO053i010p00868

Chadwick R, Boutle I, Martin G (2013) Spatial Patterns of Precipitation Change in CMIP5: Why the Rich Do Not Get Richer in the Tropics J Climate 26:3803-3822 doi:10.1175/jcli-d-12-00543.1

Chadwick R, Good P, Willett K (2016) A Simple Moisture Advection Model of Specific Humidity Change over Land in Response to SST Warming J Climate 29:7613-7632 doi:10.1175/Jcli-D-16-0241.1

Chou C, Neelin JD (2004) Mechanisms of global warming impacts on regional tropical precipitation J Climate 17:2688-2701 doi:Doi 10.1175/1520-0442(2004)017<2688:Mogwio>2.0.Co;2

Dai AG (2011) Drought under global warming: a review Wires Clim Change 2:45-65 doi:10.1002/wcc.81

Dee DP et al. (2011) The ERA-Interim reanalysis: configuration and performance of the data assimilation system Q J Roy Meteor Soc 137:553-597 doi:10.1002/qj.828

Demory ME, Vidale PL, Roberts MJ, Berrisford P, Strachan J, Schiemann R, Mizielinski MS (2014) The role of horizontal resolution in simulating drivers of the global hydrological cycle Climate Dynamics 42:2201-2225 doi:10.1007/s00382-013-1924-4

Doi T, Vecchi GA, Rosati AJ, Delworth TL (2012) Biases in the Atlantic ITCZ in Seasonal-Interannual Variations for a Coarse- and a High-Resolution Coupled Climate Model J Climate 25:5494-5511 doi:10.1175/Jcli-D-11-00360.1

Dommenget D, Floter J (2011) Conceptual understanding of climate change with a globally resolved energy balance model Climate Dynamics 37:2143-2165 doi:10.1007/s00382-011-1026-0

Dommenget D, Nice K, Bayr T, Kasang D, Stassen C, Rezny M (2019) The Monash Simple Climate Model experiments (MSCM-DB v1.0): an interactive database of mean climate, climate change, and scenario simulations Geosci Model Dev 12:2155-2179 doi:10.5194/gmd-12-2155-2019

Donat MG, Lowry AL, Alexander LV, O'Gorman PA, Maher N (2016) More extreme precipitation in the world's dry and wet regions Nat Clim Change 6:508-+ doi:10.1038/Nclimate2941

Haarsma RJ et al. (2016) High Resolution Model Intercomparison Project (HighResMIP v1.0) for CMIP6 Geosci Model Dev 9:4185-4208 doi:10.5194/gmd-9-4185-2016

He J, Soden BJ (2016) A re-examination of the projected subtropical precipitation decline Nat Clim Change 7:53-57 doi:10.1038/nclimate3157

Held IM, Soden BJ (2006) Robust responses of the hydrological cycle to global warming J Climate 19:5686-5699 doi:Doi 10.1175/Jcli3990.1

Izumi K, Bartlein PJ, Harrison SP (2015) Energy-balance mechanisms underlying consistent large-scale temperature responses in warm and cold climates Climate Dynamics 44:3111-3127 doi:10.1007/s00382-014-2189-2

Kent C, Chadwick R, Rowell DP (2015) Understanding Uncertainties in Future Projections of Seasonal Tropical Precipitation J Climate 28:4390-4413 doi:10.1175/Jcli-D-14-00613.1

Lorbacher K, Dommenget D, Niiler PP, Kohl A (2006) Ocean mixed layer depth: A subsurface proxy of ocean-atmosphere variability J Geophys Res-Oceans 111 doi:10.1029/2003jc002157

Lu J, Vecchi GA, Reichler T (2007) Expansion of the Hadley cell under global warming Geophys Res Lett 34 doi:10.1029/2006gl028443

Manabe S, Stouffer RJ (1980) Sensitivity of a Global Climate Model to an Increase of Co2 Concentration in the Atmosphere J Geophys Res-Oceans 85:5529-5554 doi:DOI 10.1029/JC085iC10p05529

Marotzke J et al. (2017) Climate research must sharpen its view Nat Clim Change 7:89-91 doi:10.1038/nclimate3206

Masson S, Terray P, Madec G, Luo JJ, Yamagata T, Takahashi K (2012) Impact of intra-daily SST variability on ENSO characteristics in a coupled model Climate Dynamics 39:681-707 doi:10.1007/s00382-011-1247-2

Mbengue C, Schneider T (2017) Storm-Track Shifts under Climate Change: Toward a Mechanistic Understanding Using Baroclinic Mean Available Potential Energy J Atmos Sci 74:93-110 doi:10.1175/Jas-D-15-0267.1

Meehl GA et al. (2007) The WCRP CMIP3 multimodel dataset - A new era in climate change research B Am Meteorol Soc 88:1383-1394 doi:10.1175/Bams-88-9-1383

Meehl GA, Stocker TF (2007) Global Climate Projections Climate Change 2007: The Physical Science Basis:747-845

Muller CJ, O'Gorman PA (2011) An energetic perspective on the regional response of precipitation to climate change Nat Clim Change 1:266-271 doi:10.1038/Nclimate1169

Muller CJ, O'Gorman PA, Back LE (2011) Intensification of Precipitation Extremes with Warming in a Cloud-Resolving Model J Climate 24:2784-2800 doi:10.1175/2011jcli3876.1

Neelin JD, Munnich M, Su H, Meyerson JE, Holloway CE (2006) Tropical drying trends in global warming models and observations P Natl Acad Sci USA 103:6110-6115 doi:10.1073/pnas.0601798103

North GR, Cahalan RF, Coakley JA (1981) Energy-Balance Climate Models Reviews of Geophysics 19:91-121 doi:DOI 10.1029/RG019i001p00091

Parry ML, Rosenzweig C, Iglesias A, Livermore M, Fischer G (2004) Effects of climate change on global food production under SRES emissions and socio-economic scenarios Global Environ Chang 14:53-67 doi:10.1016/j.gloenvcha.2003.10.008

Patz JA, Campbell-Lendrum D, Holloway T, Foley JA (2005) Impact of regional climate change on human health Nature 438:310-317 doi:10.1038/nature04188

Pendergrass AG, Gerber EP (2016) The Rain Is Askew: Two Idealized Models Relating Vertical Velocity and Precipitation Distributions in a Warming World J Climate 29:6445-6462 doi:10.1175/Jcli-D-16-0097.1

Pendergrass AG, Hartmann DL (2014) The Atmospheric Energy Constraint on Global-Mean Precipitation Change J Climate 27:757-768 doi:10.1175/Jcli-D-13-00163.1

Petoukhov V, Ganopolski A, Brovkin V, Claussen M, Eliseev A, Kubatzki C, Rahmstorf S (1999) CLIMBER-2: a climate system model of intermediate complexity. Part I: model description and performance for present climate Climate Dynamics 16:1-17

Richter I, Xie S-P (2008) Muted precipitation increase in global warming simulations: A surface evaporation perspective Journal of Geophysical Research 113 doi:10.1029/2008jd010561

Roeckner E et al. (2003) The Atmospheric General Circulation Model ECHAM5. Part 1: Model Describtion 349

Rossow W, Schiffer R (1991) Isccp cloud data products B Am Meteorol Soc 72:2-20

Sato T, Miura H, Satoh M, Takayabu YN, Wang YQ (2009) Diurnal Cycle of Precipitation in the Tropics Simulated in a Global Cloud-Resolving Model J Climate 22:4809-4826 doi:10.1175/2009jcli2890.1

Seager R, Naik N, Vecchi GA (2010) Thermodynamic and Dynamic Mechanisms for Large-Scale Changes in the Hydrological Cycle in Response to Global Warming J Climate 23:4651-4668 doi:10.1175/2010jcli3655.1

Sellers W (1969) A climatic model based on the energy balance of the earth-atmosphere system J Appl Meteorol 8:392-400

Shaffrey LC et al. (2009) UK HiGEM: The New UK High-Resolution Global Environment Model-Model Description and Basic Evaluation J Climate 22:1861-1896 doi:10.1175/2008jcli2508.1

Singh MS, Warren RA, Jakob C (2019) A Steady-State Model for the Relationship Between Humidity, Instability, and Precipitation in the Tropics J Adv Model Earth Sy doi:10.1029/2019ms001686

Stassen C, Dommenget D, Loveday N (2019) A hydrological cycle model for the Globally Resolved Energy Balance (GREB) model v1.0 Geosci Model Dev 12:425-440 doi:10.5194/gmd-12-425-2019

Stephens GL, Ellis TD (2008) Controls of Global-Mean Precipitation Increases in Global Warming GCM Experiments J Climate 21:6141-6155 doi:10.1175/2008jcli2144.1

Taylor KE, Stouffer RJ, Meehl GA (2012) An Overview of Cmip5 and the Experiment Design B Am Meteorol Soc 93:485-498 doi:10.1175/Bams-D-11-00094.1

Vecchi GA, Soden BJ (2007) Global warming and the weakening of the tropical circulation J Climate 20:4316-4340 doi:10.1175/Jcli4258.1

Vecchi GA, Soden BJ, Wittenberg AT, Held IM, Leetmaa A, Harrison MJ (2006) Weakening of tropical Pacific atmospheric circulation due to anthropogenic forcing Nature 441:73-76 doi:10.1038/nature04744

Wang Z, Myask LA (2000) A Simple Coupled Atmosphere–Ocean–Sea Ice–Land Surface Model for Climate and Paleoclimate Studies* J Climate 13:1150-1172

Weaver AJ et al. (2001) The UVic earth system climate model: Model description, climatology, and applications to past, present and future climates Atmosphere-Ocean 39:361-428

Webb MJ, Lock AP, Lambert FH (2018) Interactions between Hydrological Sensitivity, Radiative Cooling, Stability, and Low-Level Cloud Amount Feedback J Climate 31:1833-1850 doi:10.1175/Jcli-D-16-0895.1

Weller E, Jakob C, Reeder MJ (2019) Understanding the Dynamic Contribution to Future Changes in Tropical Precipitation From Low-Level Convergence Lines Geophys Res Lett 46:2196-2203 doi:10.1029/2018gl080813

Yin JH (2005) A consistent poleward shift of the storm tracks in simulations of 21st century climate Geophys Res Lett 32 doi:10.1029/2005gl023684

Tables

Table 1: List of CMIP5 models.

Models	
ACCESS1-0	ACCESS1-3
BNU-ESM	CMCC-CM
CSIRO-Mk3-6-0	FGOALS-g2
GFDL-ESM2G	GFDL-ESM2M
IPSL-CM5A-LR	MIROC-ESM-CHEM
MIROC5	MPI-ESM-LR
MPI-ESM-MR	MRI-CGCM3

Table 2: List of constants.

Variable	Dimension	Description
$c_q = -1.88$ unitless	constant	Precipitation parameter for spec. humidity
$c_{rq} = 2.25$ unitless	constant	Precipitation parameter for rel. humidity
$c_\omega = -17.69 \frac{\mathrm{s}}{\mathrm{hPa}}$	constant	Precipitation parameter for ω_{mean}
$c_{\omega std} = 59.07 \frac{\mathrm{s}}{\mathrm{hPa}}$	constant	Precipitation parameter for ω_{std}
$r_{precip} = -\frac{0.1}{24} h$	constant	Mean lifetime of water vapour
c_{eva}, c_W	constant	Evaporation efficiency
c_{turb}	constant	Turbulent wind offset for evaporation
$q_{sat-skin}$	x, y, t	Saturation pressure
r_{qviwv}	constant	Regression between atmospheric humidity and vertically integrated water vapour
T_{surf}	x, y, t	Surface temperature
u_*	x, y, t	Absolute wind climatology
z_{vapour}	constant	Scaling height of water vapour
$\vartheta_{\mathrm{soil}}$	x, y, t	Surface wetness fraction
ρ_{air}	constant	Density of air
ω_{mean}	x, y, t	Mean vertical velocity in pressure coordinates
ω_{std}	x, y, t	Standard deviation of vertical wind climatology
dt_{crcl}	constant	Model integration time step for circulation
$f = 2.5$ unitless	constant	Convergence scaling parameter
g	constant	Gravitational acceleration
q	x, y, t	Atmospheric humidity
u	x, y, t	Horizontal wind climatology
Δq_{eva}	x, y, t	Mass flux for the atmospheric humidity by evaporation
Δq_{precip}	x, y, t	Mass flux for the atmospheric humidity by precipitation

Table 3: Correlation coefficient between precipitation and vertical velocity omega (mean and daily variability) for control and the climate change response.

	Precip (control)	Omega (control)	Omega variability (control)
Change precip (full)	0.46	-0.26	-0.09
Change omega	0.16	-0.16	0.21
Change omega variability	-0.17	-0.01	-0.11

Table 4: Correlation between the external boundary forcings and the precipitation response of the sensitivity experiments.

	Change evaporation	Change omega	Change omega variability	Change precip (T_{surf})	Change precip (evaporation)	Change precip (ω)	Change precip (ω variability)
Change precip (full)	0.13	-0.58	0.45	0.58	0.38	0.75	0.73
Change evaporation		0.07	-0.24	-0.08	0.82	0	-0.16
Change omega			-0.46	0.02	0.08	-0.86	-0.49
Change omega variability				0.05	-0.27	0.5	0.68
Change precip (T_{surf})					0.19	0.07	0.19
Change precip (evaporation)						0.07	-0.02
Change precip (ω)							0.56

Table 5: Correlation between control and climate change response for the four sensitivity experiments and the change in water vapour circulation.

	Precip (control)	Omega (control)	Omega variability (control)	Change water vapour transport
Change precip (tsurf)	0.62	-0.61	0.21	1
Change precip (evaporation)	0.51	-0.17	-0.15	-0.22
Change precip (omega)	-0.03	0.18	-0.24	1
Change precip (omega variability)	0.18	-0.10	-0.08	1

List of figures

Figure 6: Precipitation response decomposition for the single RCP8.5 forcings of surface temperature (a, b), evaporation (c, d), mean circulation ω (e, f) and the daily circulation variability ω_{std} (g, h). The annual mean is shown on the left (a, c, e, g) and the seasonal cycle (JJA-DJF) on the right (b, d, f, h). The top right of each plot shows the global mean value.

Figure 7: Annual mean response of the specific humidity (a, d, g, j, m), relative humidity (d, e, h, k, n) and water vapour transport (c,f,i,l,o) for the fully forced GREB model (a-c), the single RCP8.5 forcings of surface temperature (d-f), evaporation (g-i), mean circulation ω (j-l) and the daily circulation variability ω_{std} (m-o). The top right of each plot shows the global mean value.

Figure 8: Annual mean response of the GREB model precipitation terms: moisture terms ($precip_q$ + $precip_{rq}$) (a, d, g, j, m), $precip_\omega$ (b, e, h, k, n) and $precip_{\omega std}$ (c, f, i, l, o) for the fully forced GREB model (a-c), the single RCP8.5 forcings of surface temperature (d-f), evaporation (g-i), mean circulation ω (j-l) and the daily circulation variability ω_{std} (m-o). The top right of each plot shows the global mean value.

Figure 9: Annual and zonal mean precipitation minus evaporation response for the CMIP5 RCP8.5 ensemble mean (black solid), the GREB model with all (surface temperature, evaporation, mean- and daily variability of vertical winds) forcings turned on (black dashed), the single forcing of surface temperature (red), evaporation (green), mean circulation (yellow) and circulation variability (purple) and the linear superposition of the single forcings (black circles). The x-axis is weighted by the cosine of latitude.

Figure 10: Schematic illustration of how changes in the four boundary condi- tions affect precipitation. Dashed cubes and arrows mark the control state values. Orange cubes and arrows mark changes directly forced by change in the boundary conditions. Blue cubes and arrows are resulting changes due to the response of the climate system to the forcings (orange).Panel (d) only illustrates the forced changes in precipitation (orange), but not the resulting changes (blue), as they depend on the mean circulation.

Figure S1: Seasonal cycle (JJA-DJF) response of the specific humidity (a, d, g, j, m), relative humidity (d, e, h, k, n) and water vapour transport (c, f, i, l, o) for the fully forced GREB model (a-c), the single RCP8.5 forcings of surface temperature (d-f), evaporation (g-i), mean circulation ω (j-l) and the daily circulation variability ω_{std} (m-o). The top right of each plot shows the global mean value.

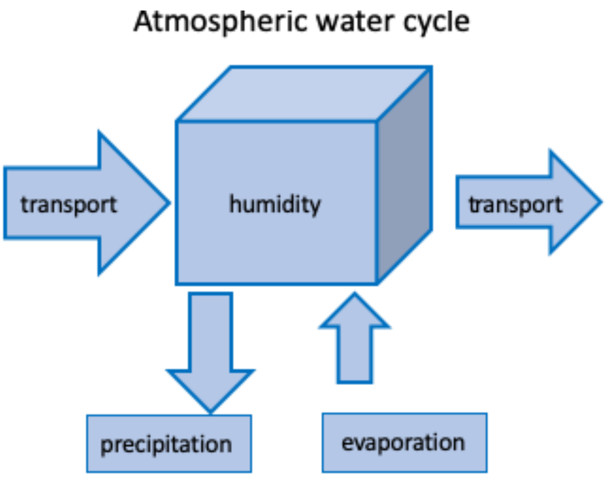

Figure 1: *GREB simplified hydrological cycle. Precipitation and evaporation do not have to be balanced locally.*

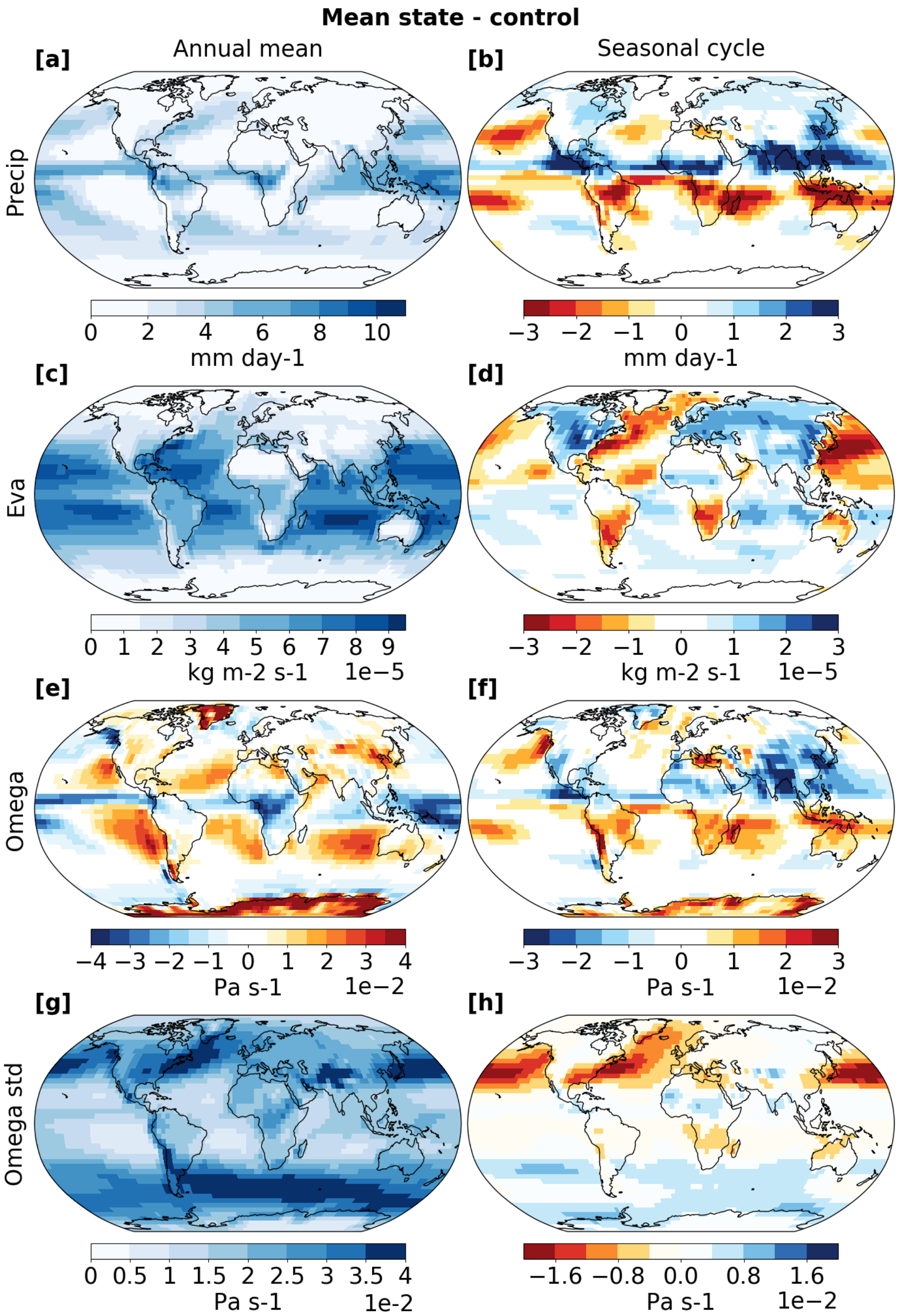

Figure 2: *GREEB control annual mean and seasonal cycle (JJA-DJF) precipitation (**a**, **b**), mean evaporation (**c**, **d**), mean vertical wind (**e**, **f**) and daily variability of vertical wind (**g**, **h**). The annual mean is shown on the left (**a, c, e, g**) and the seasonal cycle is on the right (**b, d, f, h**).*

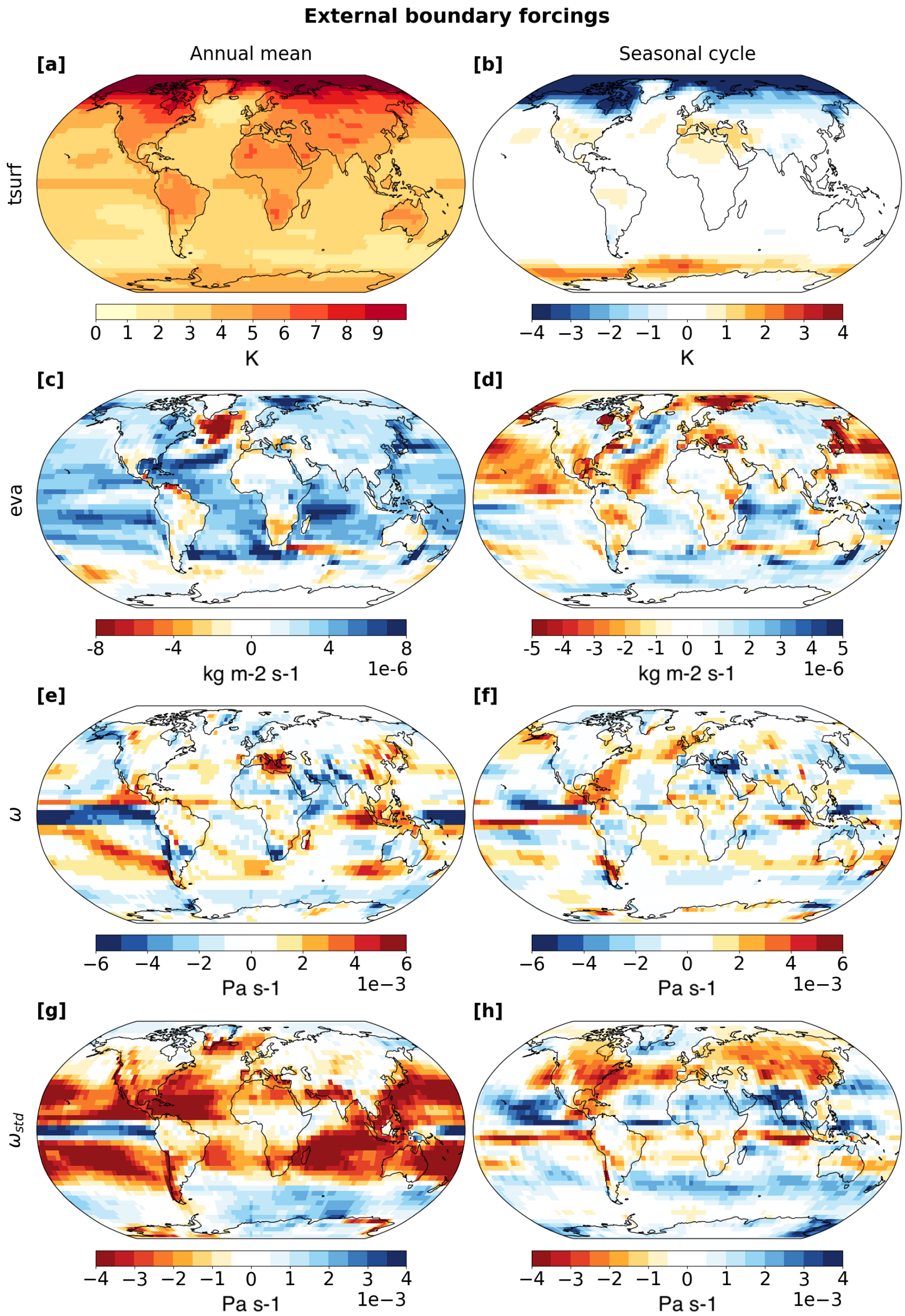

Figure 3: *CMIP5 RCP8.5 ensemble mean external boundary forcings for the GREB model of surface temperature (**a**, **b**), evaporation (**c**, **d**), mean vertical winds (**e**, **f**) and the daily variability of vertical winds (**g**, **h**). The annual mean is shown on the left (**a, c, e, g**) and the seasonal cycle (JJA-DJF) is on the right (**b, d, f, h**). Colours of the boundary forcings for evaporation, mean vertical winds and daily variability of omega have been chosen to align with the corresponding precipitation response (e.g. blue corresponds to an increase)*

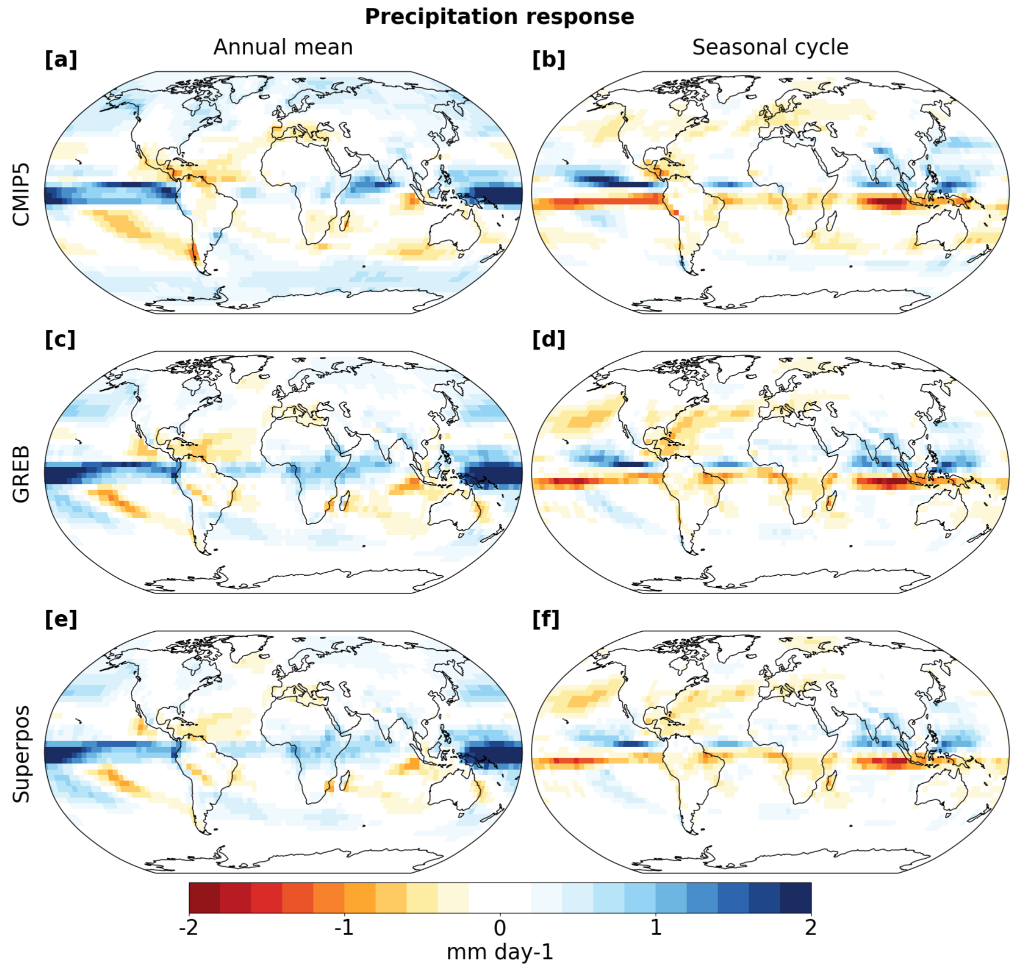

Figure 4: *Precipitation response to an RCP8.5 forcing in the CMIP5 ensemble mean (**a, b**), in the GREB model with all (surface temperature, evaporation, mean- and daily variability of vertical winds) forcings turned on (**c, d**) and the linear superposition of the single forcings (**e, f**). The annual mean is shown on the left (**a, c, e**) and the seasonal cycle (JJA-DJF) on the right (**b, d, f**).*

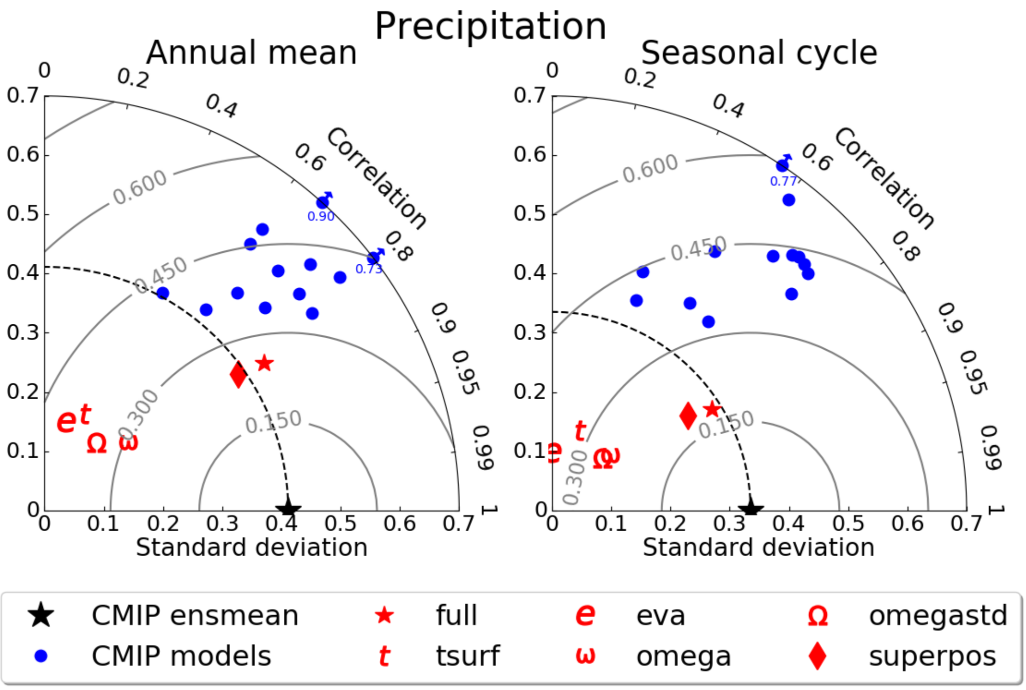

Figure 5: *Taylor diagram of the RCP8.5 precipitation response of CMIP5 models (blue), the GREB model with all (surface temperature, evaporation, mean- and daily variability of vertical winds) forcings turned on (⋆) and the linear superposition of the single forcings (♦) against the CMIP5 ensemble mean (⋆). The GREB model with single forcings of surface temperature (t), evaporation (e), mean vertical winds (ω) and daily variability of vertical winds (Ω) are also shown. The annual mean is shown on the left and the seasonal cycle (JJA-DJF) on the right. Some CMIP5 models are off the scale and indicated with a blue arrow and a number showing their standard deviation. Evaporation response is uncorrelated to the precipitation response but is the only process controlling the global mean change.*

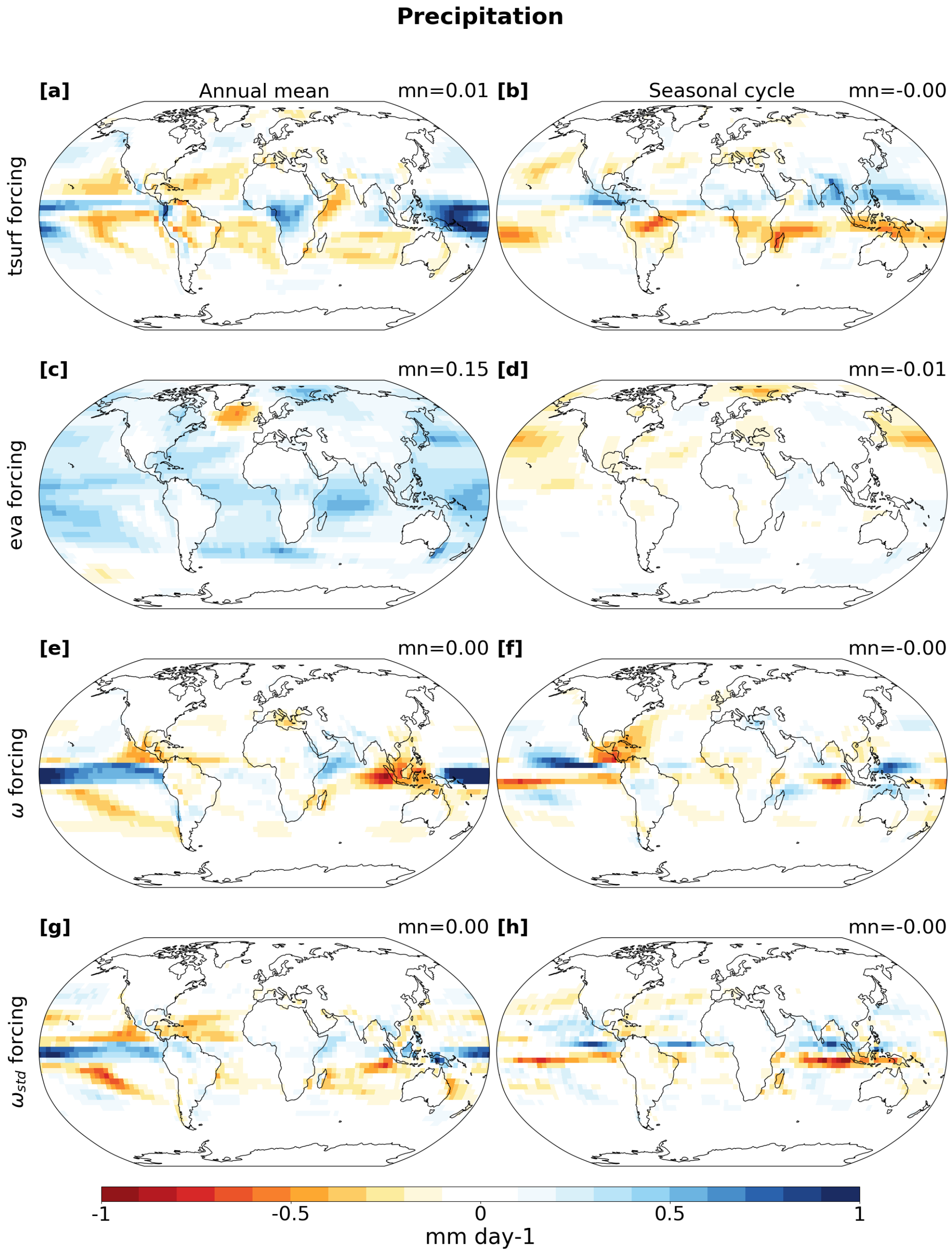

Figure 6: *Precipitation response decomposition for the single RCP8.5 forcings of surface temperature (**a, b**), evaporation (**c, d**), mean circulation* ω *(**e, f**) and the daily circulation variability* ω_{std} *(**g, h**). The annual mean is shown on the left (**a, c, e, g**) and the seasonal cycle (JJA-DJF) on the right (**b, d, f, h**). The top right of each plot shows the global mean value.*

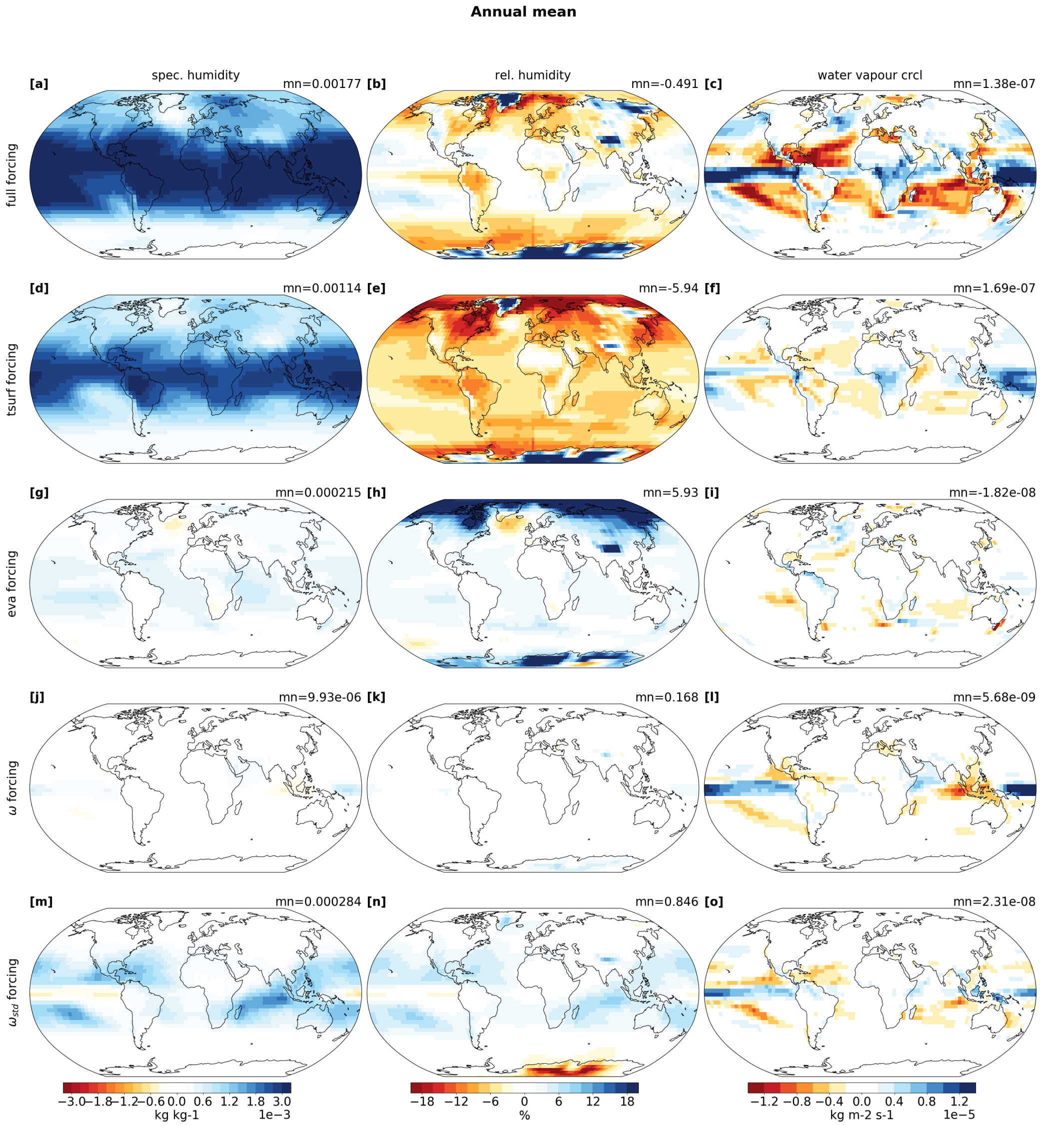

Figure 7: *Annual mean response of the specific humidity (**a, d, g, j, m**), relative humidity (**d, e, h, k, n**) and water vapour transport (**c, f, i, l, o**) for the fully forced GREB model (**a-c**), the single RCP8.5 forcings of surface temperature (**d-f**), evaporation (**g-i**), mean circulation* ω *(**j-l**) and the daily circulation variability* ω_{std} *(**m-o**). The top right of each plot shows the global mean value.*

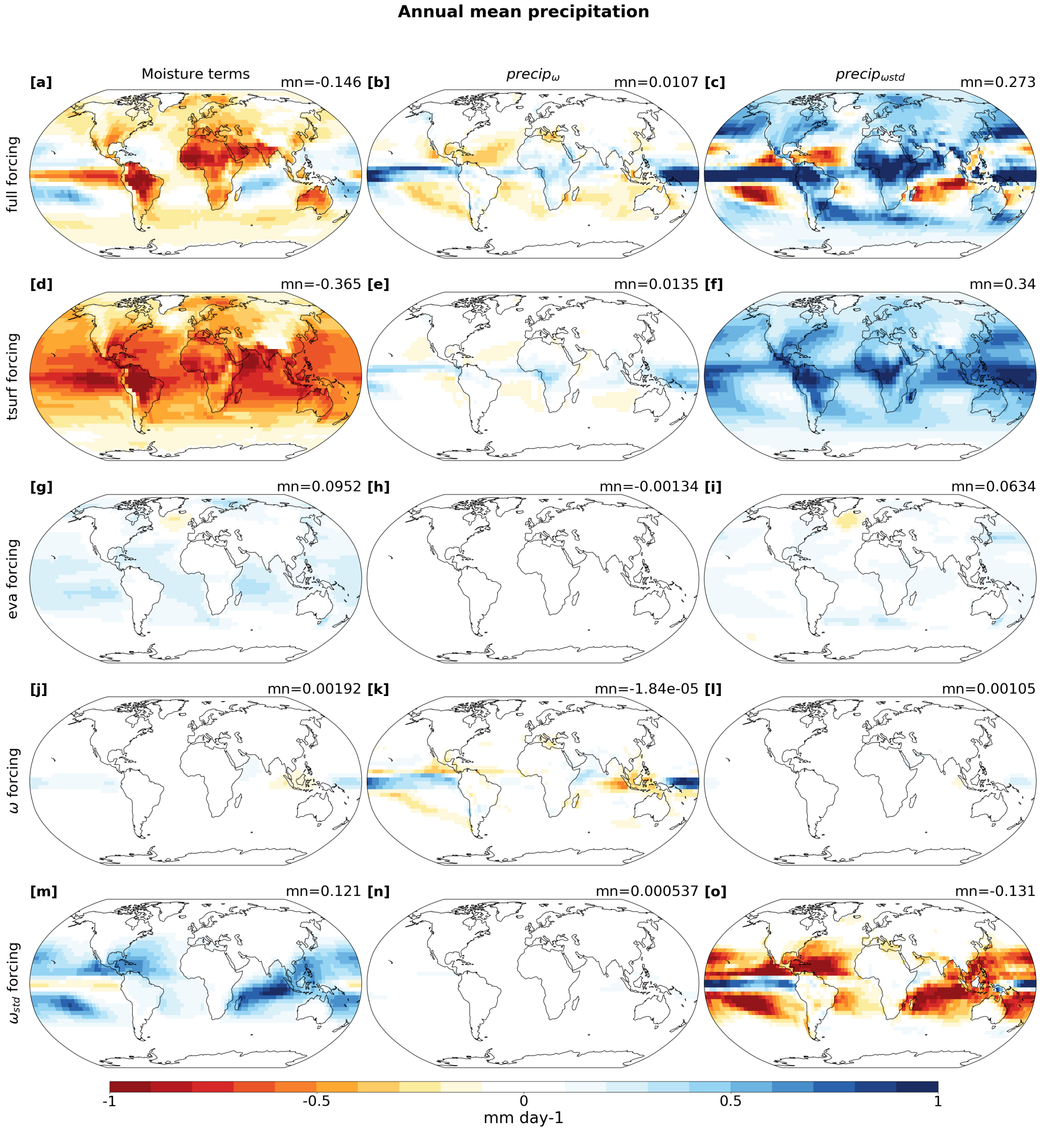

Figure 8: *Annual mean response of the GREB model precipitation terms: moisture terms (precip$_q$+precip$_{rq}$) (**a,d,g,j,m**), precip$_\omega$ (**b, e, h, k, n**) and precip$_{\omega std}$ (**c, f, i, l, o**) for the fully forced GREB model (**a-c**), the single RCP8.5 forcings of surface temperature (**d-f**), evaporation (**g-i**), mean circulation ω (**j-l**) and the daily circulation variability ω_{std} (**m-o**). The top right of each plot shows the global mean value.*

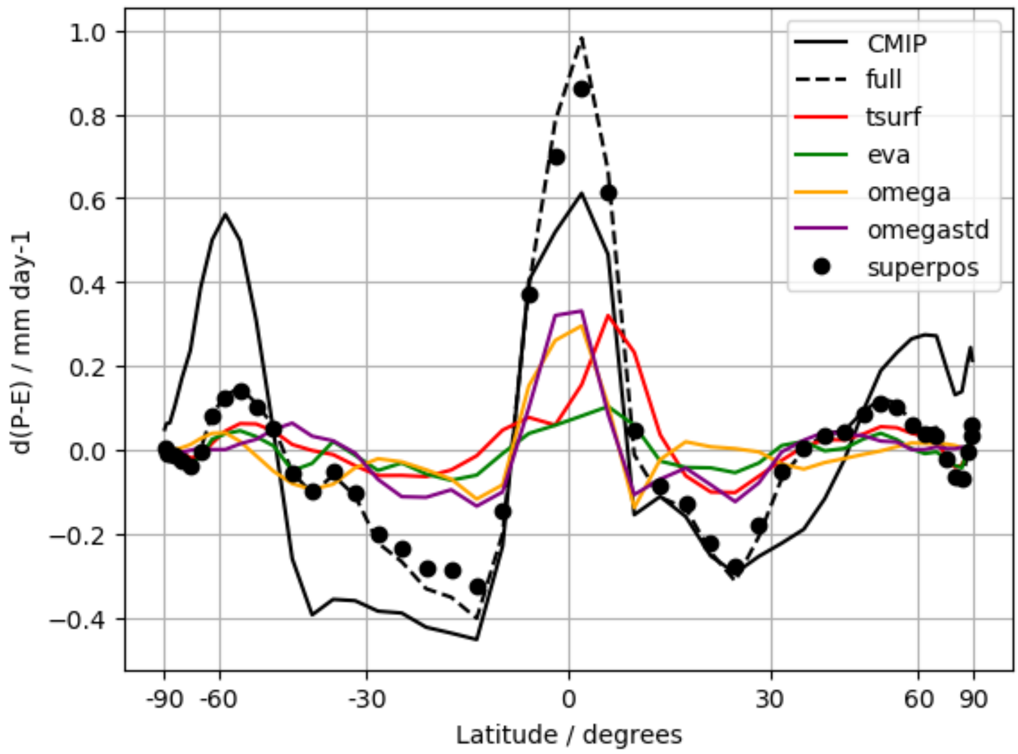

Figure 9: *Annual and zonal mean precipitation minus evaporation response for the CMIP5 RCP8.5 ensemble mean (black solid), the GREB model with all (surface temperature, evaporation, mean- and daily variability of vertical winds) forcings turned on (black dashed), the single forcing of surface temperature (red), evaporation (green), mean circulation (yellow) and circulation variability (purple) and the linear superposition of the single forcings (black circles). The x-axis is weighted by the cosine of latitude.*

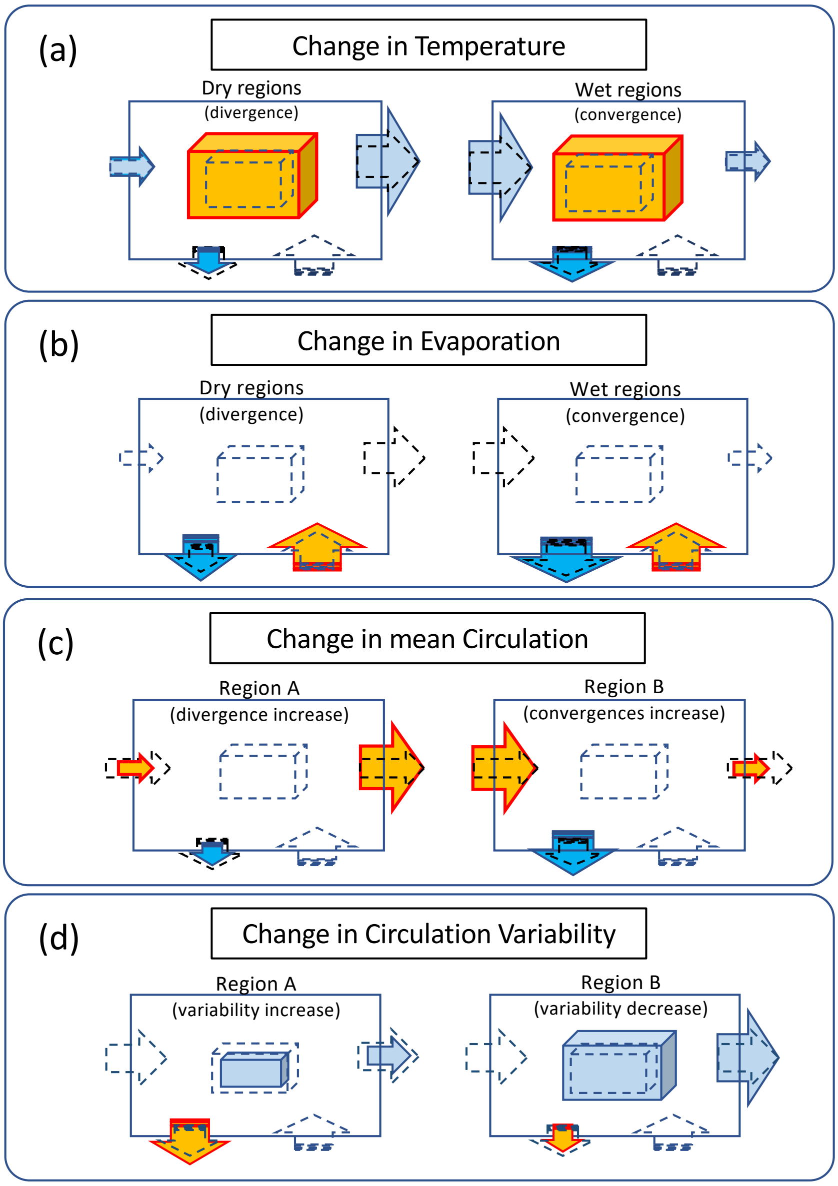

Figure 10: *Schematic illustration of how changes in the four boundary conditions affect precipitation. Dashed cubes and arrows mark the control state values. Orange cubes and arrows mark changes directly forced by change in the boundary conditions. Blue cubes and arrows are resulting changes due to the response of the climate system to the forcings (orange).Panel (d) only illustrates the forced changes in precipitation (orange), but not the resulting changes (blue), as they depend on the mean circulation.*

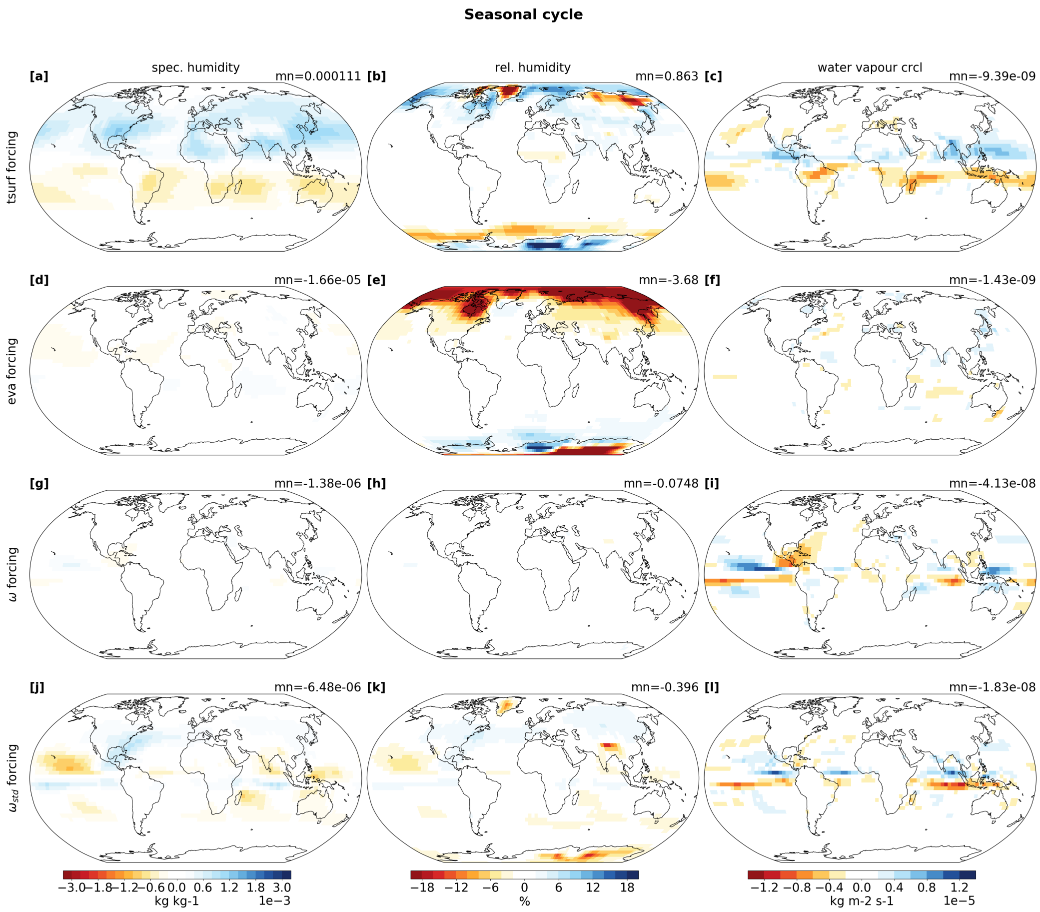

Figure S1: *Seasonal cycle (JJA-DJF) response of the specific humidity (**a, d, g, j, m**), relative humidity (**d, e, h, k, n**) and water vapour transport (**c, f, i, l, o**) for the fully forced GREB model (**a-c**), the single RCP8.5 forcings of surface temperature (**d-f**), evaporation (**g-i**), mean circulation ω (**j-l**) and the daily circulation variability ω_{std} (**m-o**).The top right of each plot shows the global mean value.*